ANALYSIS OF INTERFACIAL MICROMECHANICS OF SINGLE-FIBRE MODEL COMPOSITES USING SYNCHROTRON MICROFOCUS X-RAY DIFFRACTION

Y. T. Shyng, R. J. Young and R. J. Davies*

Manchester Materials Science Centre, UMIST/University of Manchester,
Grosvenor St., Manchester, M1 7HS, UK
*European Synchrotron Radiation Facility, B.P. 220, F-38043, Grenoble Cedex, France

ABSTRACT

Synchrotron radiation was used in this study in order to obtain high quality diffraction patterns of poly(*p*-phenylene terephthalamide) (PPTA) and poly(*p*-phenylene benzobisoxazole) (PBO) fibres. Model single-fibre composites were made for the purpose of interfacial shear stress (ISS) analysis. Shifts of meridional Bragg peaks as a function of stress were determined and the fibre crystal modulus values obtained were 224 GPa for the PPTA fibre and 469 GPa for the PBO fibre. The variation of stress was mapped along the fibre in the composites. A mathematical spline fit method was used with the force balance approach that then gave realistic interfacial shear stress values.

1. INTRODUCTION

The origin of poly(*p*-phenylene benzobisoxazole) (PBO) fibre can be traced back to the late 1960s while the U. S. Air Force was researching for a new man-made fibre material with good mechanical properties and heat resistance [1]. Due to the rigid-rod form of its molecular structure as illustrated in *Figure 1(a)*, the PBO fibre possesses outstanding mechanical properties, long-term stability, and excellent tolerance of high temperature. Currently it is commercialized under the trade name Zylon™.

The poly(*p*-phenylene terephthalamide) (PPTA) fibre was first developed by the Du Pont Company in 1965 and then commercialized in 1972 as Kevlar™. The molecular structure of PPTA fibres is shown in *Figure 1(b)*. Initially the Kevlar fibre was designed as a composite reinforcement material, but has since been widely applied to many applications [2]. Recently TEIJIN has commercialized a new PPTA fibre under the trade name of Twaron™. *Table 1* provides a comparison between the physical properties of PBO and PPTA fibres.

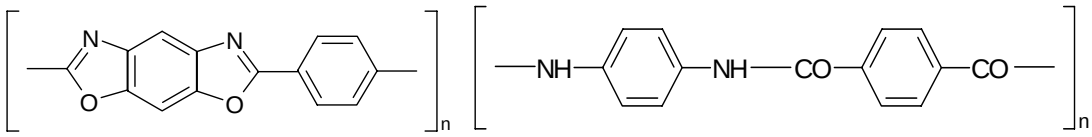

(a) *(b)*

Figure 1. Structures of (a) PBO and (b) PPTA fibres

The interfacial strain/stress distributions of a single-fibre model composite have been studied extensively, and the most common technique applied in this field has been Raman spectroscopy [3]. Based on the corresponding Raman band shift rate as a calibration, the

stress and strain distributions along a fibre and the shear stress at the interface can be calculated.

Table 1. Typical properties of PBO and PPTA fibres

	Density (g/cm^3)	Tensile Strength (GPa)	Tensile Modulus (GPa)	Maximum Strain (%)
PBO	1.56	5.8	280	2.5
PPTA	1.40	3.5	130	3.3

This Raman spectroscopy approach has several limitations however. Firstly, it is essential that the matrix is either transparent or at least partially transparent in order to allow the laser beam to penetrate the resin. The use of opaque matrices is therefore precluded, such as the widely used engineering plastics PP (polypropylene) and PEEK (polyetheretherketone). Secondly, it has been reported that a thermal effect exits for Raman spectroscopy [4]. This thermal effect is induced by the high-energy laser which transfers energy to the sample, consequently affecting the spectra peak positions.

Synchrotron radiation has been proven as a powerful tool for studying the structure of high performance polymer fibres such as PBO and PPTA, and the structural changes they undergo during deformation [5]. It is well known that their so-called “rigid-rod” molecular structures are able to sustain a high tensile load for a relatively low elongation. Furthermore, the well-packed and highly crystalline structures of these fibres give strong and well-defined X-ray diffraction (XRD) patterns, therefore making them ideal for XRD studies.

In this study, single-fibre embedded model composites were examined by synchrotron radiation at beamline ID13 of the European Synchrotron Radiation Facility (ESRF). The stress distributions along the fibres were mapped and the corresponding interfacial shear stress values calculated.

2. EXPERIMENTAL

2.1. Materials

The PBO and PPTA fibres investigated in this study were supplied by TOYOBO, Japan, and TEIJIN, Japan, respectively. Both fibre types are produced commercially under the trade names of Zylon^{TM} (PBO) and Twaron^{TM} (PPTA). A Philips 525M scanning electron microscope (SEM) was used to determine fibre diameters. At least 20 fibres of each type were randomly selected and then examined at three different magnification levels. Average diameters and standard deviations were calculated for each fibre type with accuracy ensured through SEM calibration using a standard sample.

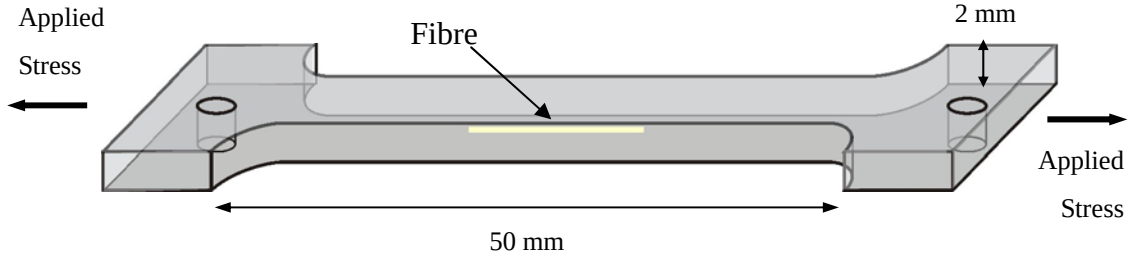

Figure 2. Illustration of single-fibre embedded sample

Single-fibre embedded model composites were prepared using a rectangular mould. The chosen matrix material was a cold-curing two-part epoxy resin supplied by Ciba Geigy, UK. It consisted of 100 parts by weight of butane-1,4-diol diglycidyl ether resin (LY5052) and 38 parts by weight of isophorone diamine hardener (HY5052). While the epoxy resin mixture filled the mould, a single straight fibre was inserted to form an embedded composite. The epoxy was then cured at room temperature for seven days before being cut into strips and shaped into dumb-bell test specimens, as shown in *Figure 2*.

2.2. X-ray diffraction methods

The x-ray micro-diffraction experiments were conducted at the European Synchrotron Radiation Facility (ESRF) on beamline ID13. The beamline was configured with a Kirkpatrick-Baez (KB) type mirror and collimated using a piezo-based block collimation system. This provided an on-sample beam spot-size of approximately 5 μm with a radiation wavelength of 0.095 nm. A MARCCD detector with an average pixel size of 257.79 μm² was used to capture diffraction patterns. All patterns were taken using an exposure time of 10 s. The sample-to-film distance was calculated from the diffraction pattern of an Al_2O_3 calibration sample and was determined to be 143.17mm of PPTA and 103.15 mm of PBO composites.

A 'Minimat' rig with an on-board load cell was used for sample deformation which allowed the *in situ* load applied to the sample to be recorded. The samples were fixed to the rig using a grip mechanism with additional screws to avoid slippage. Deformation was applied to the samples using a manually controlled gearbox. Diffraction patterns were generated along the embedded fibre length at various levels of sample loading and at 25 μm and 20 μm intervals of PPTA and PBO composite respectively.

2.3. Calculation of crystal strain and crystal modulus

Analysis of the diffraction data was performed using the FIT2D software application [6][7]. Radial profiles were first generated which allowed the positions of the fibre meridional reflections to be determined. This enables the subsequent calculation of lattice spacings in the fibre axis direction (commonly refered to as *c*-spacing). This was calculated using 1-dimensional diffraction grating theory according to *Equation 1* [8]. A more detailed description of a similar analysis procedure has previously been reported elsewhere [9].

$$c = \frac{n\,\lambda}{\sin\left[\tan^{-1}\left(\frac{x}{r}\right)\right]} \tag{1}$$

where n is the order of diffraction, λ is X-ray wavelength, r is the sample-to-film distance, and x is the reflection distance from beam centre. Crystal strain (ε_c) may then be calculated as the change in lattice spacing during sample deformation using *Equation 2*.

$$\varepsilon_c = \frac{c_0 - c_\sigma}{c_0} \tag{2}$$

where c_0 is *c*-spacing determined from the undeformed sample whilst c_σ is *c*-spacing determined from the sample at σ stress level. The calculation of crystal modulus (E_c) may also be performed according to *Equation 3* where σ is a given level of fibre stress. For such

calculations it is necessary to assume that stresses acting upon crystallite domains within the fibres are the same as macroscopic fibre stress.

$$E_c = \frac{\sigma}{\varepsilon_c} \tag{3}$$

2.4. Calculation of interfacial shear stress

According to the force balance approach, the interfacial shear stress of a fibre embedded inside a matrix can be measured by dividing the fibre into small segments [10], as illustrated in *Figure 3*.

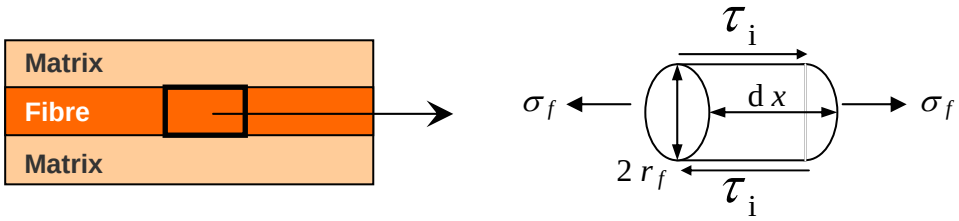

Figure 3. Fibre segment of a single fibre embedded model composite [10]

where r_f is the fibre radius, dx is the segment length and σ_f is the axial fibre stress. Therefore, interfacial shear stress of the segment τ_i can be expressed as shown in *Equation 4*.

$$\tau_i = \frac{r_f}{2}\frac{\mathrm{d}\,\sigma_f}{\mathrm{d}\,x} \tag{4}$$

It is evident that by obtaining a value for dσ_f /dx from the diffraction data generated, interfacial shear stress may be calculated. A mathematical spline fit enables this value to be determined and additionally provides an effective way to transform the original dσ_f /dx data into a smooth line form.

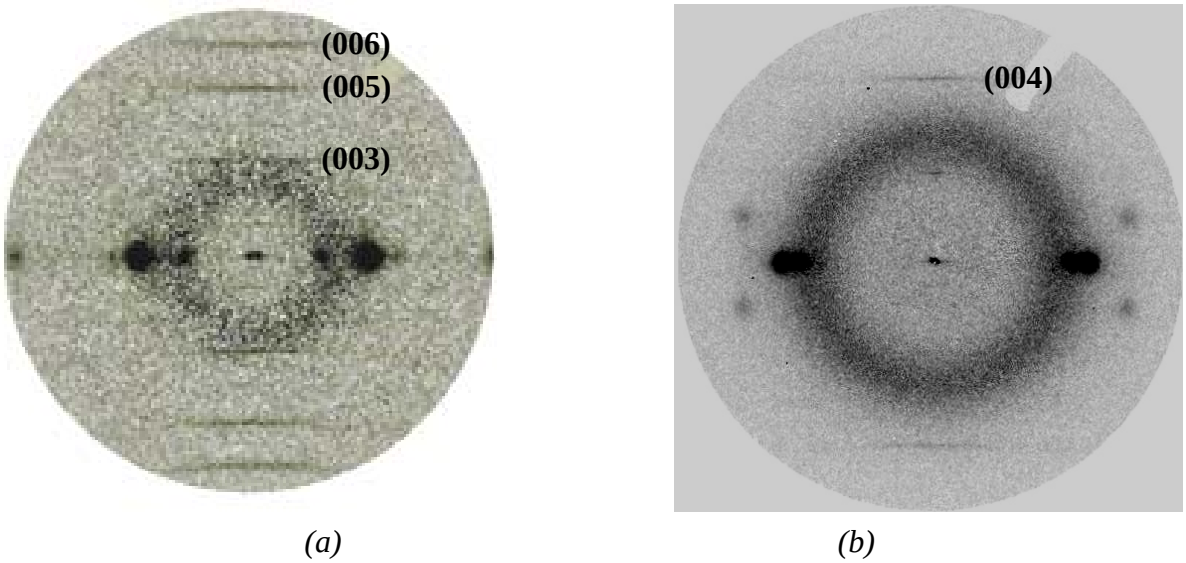

(a) *(b)*

Figure 4. Synchrotron diffraction patterns (a) PBO and (b) PPTA fibres

3. RESULTS AND DISCUSSION

3.1. Determination of fibre diameter

The average value of fibre diameter and its standard deviation are 11.2 ± 0.7 μm and 12.1 ± 0.5 μm for the PBO and PPTA fibres respectively.

3.2. Single-fibre stress calibration

Figure 4 shows typical diffraction patterns for the PBO and PPTA fibres used in this study. The PBO diffraction pattern exhibits well-defined (003), (005) and (006) layer lines whilst only the (004) layer line is easily visible in the PPTA diffraction pattern.

The results of stress calibration and crystal modulus determination for PBO and PPTA fibres are shown in *Figure 5*. It is calculated that PBO fibre has a crystal modulus of 469 GPa, which is in good agreement with previous studies [5,8]. PPTA fibre calculated crystal modulus is reported to be approximately 220 - 290 GPa [11], which is also consistent with the 224 GPa result obtained in this study. The stress calibrations obtained in *Figure 5* may also be used to relate applied stress to crystal strain and so form a calibration for the embedded fibre samples.

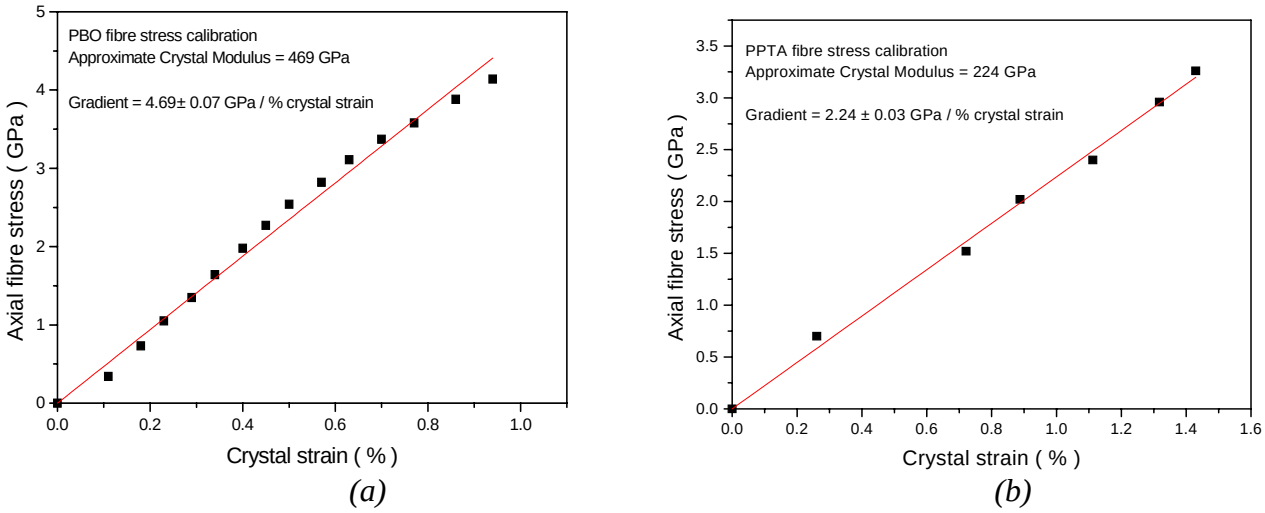

Figure 5. Fibre stress calibrations of (a) PBO and (b) PPTA fibres

3.3. PPTA composite ISS analysis

The variation of axial fibre stress in a PPTA fibre embedded model composite and its spline fit results are shown in *Figure 6*. The position values along the fibre refer to the distance in microns from the free fibre end. The diffraction data were generated at four different levels of loading. The initial stress of approximately 0.05 GPa in the unloaded specimen is possibly due to pre-stretching of the fibre during insertion. The axial fibre stress induced by deformation of the model composite increased to plateau values of approximately 0.5 GPa, 0.95 GPa and finally 1.2 GPa.

The fitted lines in *Figure 6* represent the results of spline fits. As mentioned previously, the spline fit results give a smooth estimation of axial fibre stress variation along the fibre and provide a $d\sigma_f$ /dx distribution for use in the shear-lag equation. This axial fibre stress distribution is in good consistency with the traditional shear-lag model. As the load applied to the sample was relatively low the interface between the PPTA fibre and the epoxy matrix was

fully bonded throughout the entire deformation process.

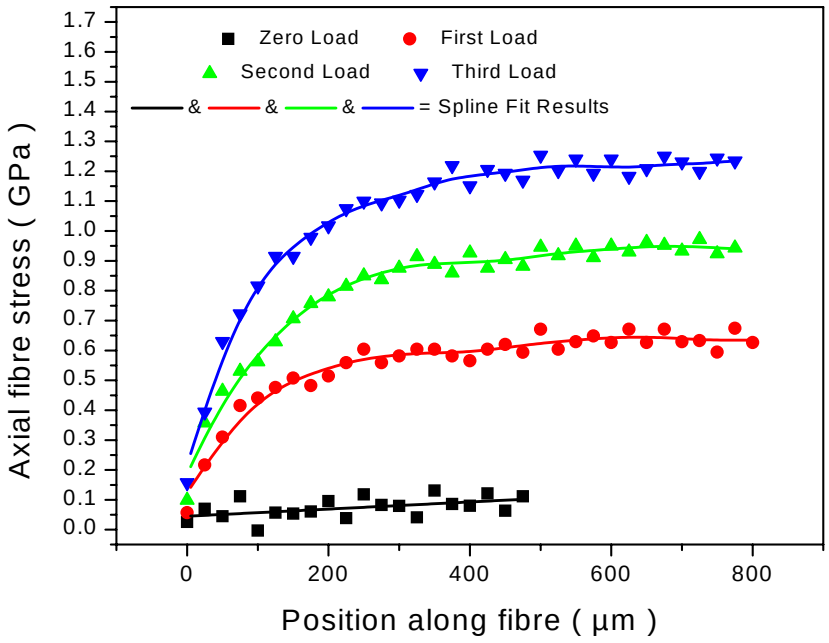

Figure 6. Stress along a PPTA fibre embedded in an epoxy resin matrix subjected to increasing levels of loading

Figure 7 shows the variation of interfacial shear stress with position along the embedded PPTA fibre. The highest interfacial shear stress is at the free end of the fibre (0 µm position), gradually decreasing to zero with increasing distance from the free fibre end. The maximum interfacial shear stress depends upon the loading level. At zero load it is 0 MPa, increasing to 11 MPa, 15 MPa and 22 MPa as the load is increased.

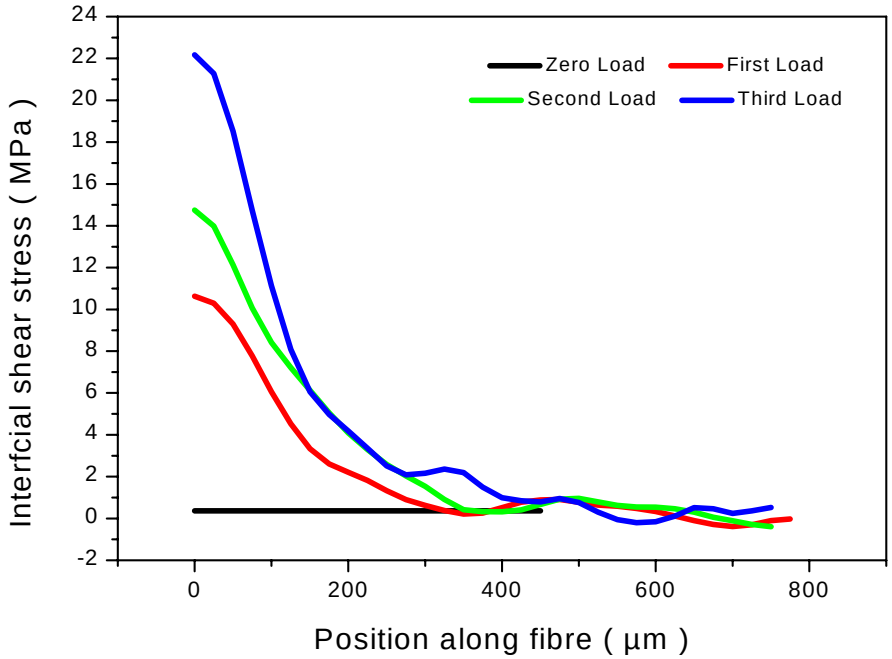

Figure 7. Interfacial shear stress versus fibre length for embedded PPTA fibre determined from the spline fitting

It was previously observed that the interface is fully bonded along the fibre length and the interfacial shear stress results provide further conclusive agreement of this. The fluctuations in interfacial shear stress evident towards the centre of the fibre (>200 µm) might be caused, at least partially, by the parameter adjustment during the spline fitting process.

3.4. PBO composite ISS results

Figure 8 shows the axial fibre stress distribution in a PBO fibre model composite and the spline fit results. It shows a similar profile to that shown in *Figure 6* for the PPTA fibre. It has a slightly higher initial stress of approximately 0.1 GPa and the axial maximum fibre stresses induced by sample deformation are 0.9 GPa, 1.4 GPa and at 2.0 GPa at the highest load level.

Figure 9 shows the variation in interfacial shear stress with position along the embedded PBO fibre. It also exhibits a profile similar to that of the PPTA sample, which indicates the PBO composite to also have a fully bonded interface. Unlike the PPTA results however, the interfacial shear stresses in the PBO model composite sample are higher, being approximately 17.5 MPa, 22 MPa and 30 MPa at the highest loading level. This is due to the much higher crystal modulus of the PBO fibre type.

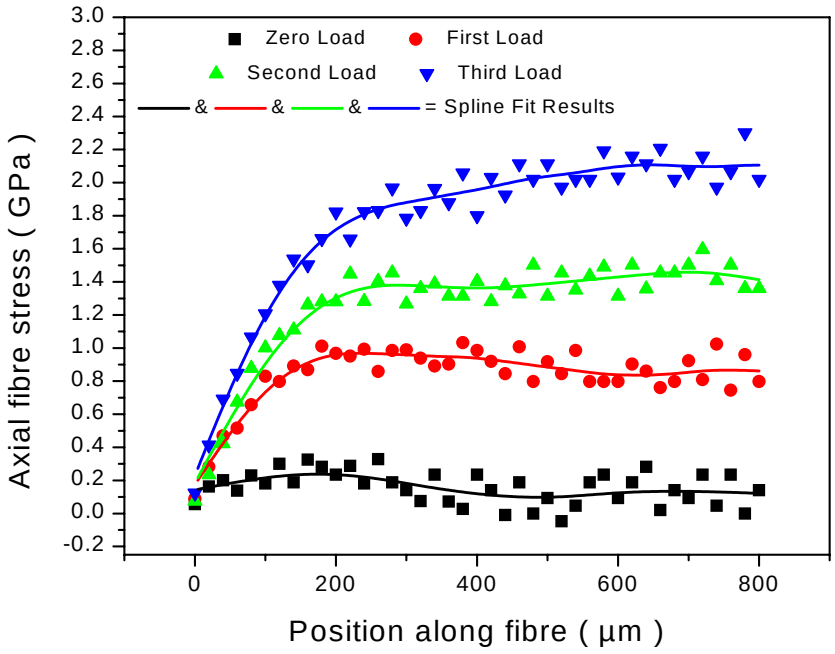

Figure 8. Stress along a PBO fibre embedded in an epoxy resin matrix subjected to increasing levels of loading

The interfacial shear stresses in the PBO model composite show similar fluctuations as observed in the PPTA sample towards the centre of the fibre (>200 µm). In this case however, the fluctuations occur over a wider range which can be explained by examination of with the original axial fibre stress data. It can be seen that the PBO data exhibits a much higher degree of scattering than the similar PPTA data.

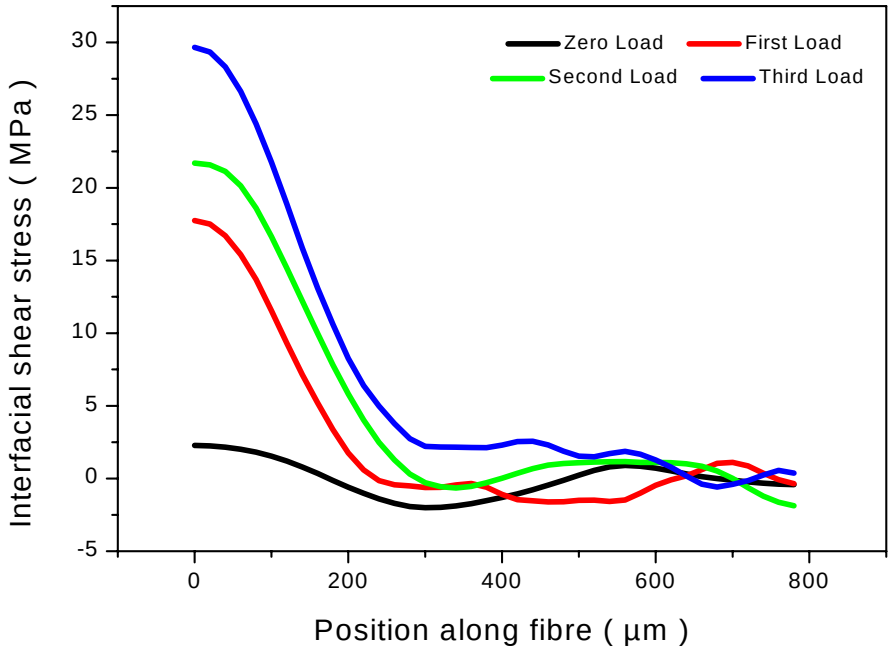

Figure 9. Interfacial shear stress versus fibre length for embedded PBO fibre determined from the spline fitting

4. CONCLUSIONS

High quality diffraction patterns of single rigid-rod polymer fibres such as PPTA and PBO can be obtained using synchrotron radiation. The stress calibrations generated in this study are similar to previous studies and the interfacial shear stress analyses give further confirmation of the feasibility of this synchrotron radiation approach.

Furthermore, due to the nature of synchrotron radiation, diffraction patterns can be obtained regardless of the type of matrix that is employed, which is the primary obstacle in Raman spectroscopy analysis. Without the concern of matrix type, different matrix materials that are not transparent, such as polyetheretherketone (PEEK) and polypropylene (PP), will be examined in subsequent studies.

ACKNOWLEDGEMENTS

The authors would like to express their thanks to Manfred Burghammer at ID13 for assistance with the experimental setup, and Toyobo and Teijin for supplying fibre samples. Our thanks also extend to Andrew Hammersley for use of the FIT2D software application and colleagues in the Manchester Materials Science Centre who have collaborated with us in this study.

REFERENCES

1. De Lange, P. J., Mäder, E., Mai, K., Young, R. J. and Ahmad, I., “Characterisation and micromechanical testing of the interphase of aramid reinforced epoxy composites”, Composites A: Applied Science and Manufacturing, 32 (2001), 331-342
2. Yang, H. H., Kevlar Aramid Fiber, John Wiley & Sons (1993)
3. So, C. L., Bennett, J. A., Sirichaisit, J. and Young, R. J., “Compressive behaviour of rigid-rod polymer fibres and their adhesion to composite matrices”, Plastics, Rubber and Composites, 32 (2003) 199-205

4. Banwell, C. N. and McCash, E. M., Fundamentals of Molecular Spectroscopy Fourth Edition, The McGraw-Hill Companies (1994)
5. Montes-Morán, M. A., Davies R. J., Riekel C. and Young R. J., "Deformation studies of single rigid-rod polymer-based fibres. Part 1. Determination of crystal modulus", Polymer, 43 (2002), 5219-5226
6. Hammersley, A. P. and Riekel, C., "MFIT: Multiple Spectra Fitting Program", Synchrotron Radiation News, 2 (1989), 24
7. Hammersley, A. P., "FIT2D: an introduction and overview", ESRF Internal Report, ESRF97HA02T (1997)
8. Davies R. J., Montes-Morán, M. A., Riekel C. and Young R. J., "Single fibre deformation studies of poly(*p*-phenylene benzobisoxazole fibres. Part 1: determination of crystal modulus", J. Mater Sci, 36 (2001), 3079-3087
9. Young, R. J. and Lovell, P. A., Introductions to Polymers, second edition, Chapman & Hall (1996)
10. McCrum, N. G., Buckley, C. P., Bucknall, C. B., Principles of Polymer Engineering, Oxford University Press (1997)
11. Rutledge, G. C. and Suter, U. W., Calculation of mechanical properties of poly(*p*-phenylene terephthalamide) by atomistic modeling, Polymer, 32 (1991), 2179